Vol. 18, No. 1 (2019) 165-180
Revista Mexicana de Ingeniería Química

EFFECT OF TWO-FLUID NOZZLES ON THE STABILITY CHARACTERISTICS OF EMULSIONS PREPARED BY A HIGH-ENERGY METHOD (MICROFLUIDIZATION)

EFECTO DE BOQUILLAS NEUMATICAS DE DOS FLUIDOS EN LAS CARACTERÍSTICAS DE ESTABILIDAD DE LAS EMULSIONES ELABORADAS CON MÉTODO DE ALTA ENERGÍA (MICROFLUIDIZACIÓN)

J.C. Villalobos-Espinosa[1], M.X. Quintanilla-Carvajal[2], V.G. Granillo-Guerrero[1], L. Alamilla-Beltrán[1], H. Hernández-Sánchez[1], M.J. Perea-Flores[3], E. Azuara-Nieto[4], G.F. Gutiérrez-López[1]*

[1]*Instituto Politécnico Nacional, Departamento de Ingeniería Bioquímica; Doctorado en Ciencias en Alimentos; Escuela Nacional de Ciencias Biológicas, Carpio y Plan de Ayala S/N Santo Tomás, Código Postal 11340 Ciudad de México, México.*

[2]*Facultad de Ingeniería, Universidad de La Sabana, Km 7 vía autopista Norte, Bogotá, Colombia.*

[3]*Laboratorio de Microscopía Confocal; Centro de Nanociencias y Micro y Nanotecnología, Unidad Profesional Adolfo López Mateos, Instituto Politécnico Nacional, Luis Enrique Erro S/N, Zacatenco, Código Postal 07738, Ciudad de México, México.*

[4]*Instituto de Ciencias Básicas de la Universidad Veracruzana, Calle Dr. Luis Castelazo Ayala S/N, Colonia Industrial Animas, Xalapa, Veracruz, México.Código Postal 91190*

Received: May 09, 2018; Accepted: June 04, 2018

Abstract

The atomization of oil in water emulsions is used in the food industry in the preparation of several products. Its passage through the atomization devices could have an influence on the stability of the emulsion and, consequently on the final product. In the present work, it was evaluated the influence of two fluid nozzles of different dimensions and geometry on stability parameters of oil in water emulsion produced by microfluidization and by using gum Arabic as wall material. Results indicated that the droplet size, the polydispersity index and the Turbiscan stability index of atomized emulsions were affected by an initial destabilization which caused their increment with time. It was found that, atomized emulsions presented Oswald ripening rates more pronounced than original emulsion which possibly included diffusion-interfacial tension compensation. The confocal laser scanning microscopy images confirmed that the passage of the emulsion through the atomization devices decreased the thickness of wall material of the droplets with respect to the original emulsion which strongly influenced the destabilization of emulsions due to decreased coverage and polar-non-polar disruption. It was concluded that, in the design of products prepared by atomization, the stability of the atomized emulsions must be considered by including a proper selection of the atomizer and possibly, a suitable liquid sampling-characterization on-line scheme.

Keywords: atomization, two-fluid nozzle, oil in water emulsions, stability, Ostwald ripening.

Resumen

La atomización de emulsiones aceite en agua se usa en la industria alimentaria en la preparación de diversos productos. Su paso a través de dispositivos de atomización podría influir en su estabilidad y, por consiguiente, en el producto final. En este trabajo, se evaluó la influencia de dos boquillas de dos fluidos de diferentes dimensiones y geometrías sobre los parámetros de estabilidad de emulsiones aceite en agua elaboradas por microfluidización, utilizando goma Arábiga como material de pared. Los resultados mostraron que el tamaño de gota, el índice de polidispersidad y el índice de estabilidad del Turbiscan de las emulsiones atomizadas se vieron afectados por una desestabilización inicial que dio lugar a que, los mismos, se incrementaran con el tiempo. Se encontró que las emulsiones atomizadas mostraron una maduración de Ostwald que incluyó, posiblemente, compensación de mecanismos de difusión-tensión interfacial más pronunciada que la original. Las imágenes obtenidas con el microscopio confocal de barrido láser confirmaron que el paso de la emulsión a través de los dispositivos de atomización disminuyó el espesor del material de pared de las gotas con respecto a la emulsión original, lo que influyó en la desestabilización de las emulsiones debido a una menor cobertura y consecuente perturbación del balance entre grupos polares y no polares. Se concluyó que en el diseño de los productos elaborados por aspersión de emulsiones deben considerarse la estabilidad del líquido atomizado, una selección apropiada del atomizador y, posiblemente, un sistema de muestreo y caracterización de los fluidos en línea.

Palabras clave: atomización, boquilla neumática de dos fluidos, emulsiones aceite en agua, estabilidad, maduración de Ostwald.

* *Corresponding author. E-mail*: gusfgl@gmail.com

doi: https://doi.org/10.24275/uam/izt/dcbi/revmexingquim/2019v18n1/Villalobos
issn-e: 2395-8472

1 Introduction

Emulsions consist of two or more immiscible liquids, forming two phases, one being dispersed into the other in the form of droplets (McClements and Jafari, 2018) and are widely used ingredients in the food industry, either as an intermediate product within a manufacturing scheme or as a final product (McClements 2007; Owaga *et al*., 2003; Tadros 2013). To stabilize oil droplets in an aqueous media, wall materials and surfactants are used. Gum Arabic (GA) has been widely applied as wall material (Taherian *et al*., 2008) due to its surface activity in the formulation of oil in water emulsions. The adsorption of the biopolymers at the oil-water interface gives rise to interfacial membranes, which reduce the contact area between oil molecules and water.

The protein part (~ 2%), of the gun Arabic adsorbs on the oil-water interface (Wang, *et al*., 2011) and stabilize the oil in water emulsions, by forming a membrane (wall material) around the droplets of the emulsion. At the same time, this interfacial membrane can serve as a barrier material for microencapsulated systems.

In general, the stabilizing and barrier properties of biopolymers in foods are determined by their molecular weight, conformation, flexibility, polarity and interactions (McClements, 1999). Gum Arabic presents carboxyl groups composed by: L-rhamnose (~ 13%), D-galactose (~ 40-44%), L-arabinose (~ 24-27%) that can exhibit a large dissociation, resulting in Coulomb repulsions of negatively charged carboxyl groups, which can cause the molecule to adopt an expanded and highly charged structure (Whistler, 2012).

The process of transforming the mixture of two immiscible liquids into an emulsion or, of reducing the droplet size of a pre-existing emulsion is known as homogenization (McClements, 2015; Hakansson and Rayner, 2018). During microfluidization (MF) (high shear homogenization), the reduction in droplet size is carried out in the interaction chamber(s) due to forces of deformation and high-speed collisions of the mixture of immiscible fluids with the metal walls of the chamber and between the liquid streams themselves (Jafari *et al*., 2007; Villalobos-Castillejos *et al*., 2018), thus producing smaller sizes of droplet and a more homogeneous distribution of the dispersed phase (Jafari *et al*., 2007b).

Oil in water emulsions are often subjected to atomization as in the formation of edible films, preparation of capsules by spray drying, preparation of films, manufacturing of coatings, addition of a number of food additives to different food matrices among others (Fuentes-Ortega *et al*., 2017; Kanellopoulos *et al*., 2017; Haffner *et al*., 2016) and, the properties of the emulsions are usually related to those of the obtained final product without considering that, during their passage through the atomization device, the emulsions may undergo changes due to the high shear stress applied and which may have an influence on the properties of the emulsion that is fed to the atomization device.

The atomization of emulsions is a commonly used stage in various processes and industrial areas such as food, pharmaceutical, automotive, metal, etc. and is defined as the disintegration of a liquid in the form of drops (Wang *et al*., 2014; Aliseda *et al*., 2008; Hede *et al*., 2008). However, the passage of the emulsion through the atomizing device and atomization might have an influence on the properties of the emulsion and the characteristic of the final product, such as stability, droplet size, structure, shape and distribution of the compounds could be affected. An adequate liquid dispersion into droplets depends on the type of atomizing device and on the stability features of the emulsion (Foerster *et al*., 2016).

Munoz-Ibanez *et al*. (2015) determined the changes in emulsion droplet size and polydispersity due to nozzle and disc atomization as well as the influence of the viscosity of the dispersed phase on the effects that the atomizing device had in oil in water emulsions and mentioned that the initial droplet size, atomization energy applied and the viscosity ratio between dispersed and continuous phases were identified as the key factors that determined the emulsion characteristics after atomization.

The study of stability related parameters of the final, atomized emulsion, could provide useful data for assessing on the selection of the type of atomizer, as well as on the structure-function properties of the end product in relation to the fed emulsion that gave place to such product. The objective of this work was to determine the influence of two nozzles with external mixing on stability related parameters of oil in water emulsion prepared by microfluidization.

2 Materials and methods

2.1 Core and wall materials

All emulsions were prepared by using deionized water, gum Arabic (GA) (Gum Arabic E-414 Quich gum NOREVO) as wall material, and commercial corn oil (CO) (MAZOLA, ACH Foods Mexico, SA de CV, Ciudad de Mexico) as the core substance.

2.2 Preparation of pre-emulsions

The gum Arabic was dissolved in type I water (at 25% of solids %(w/w)), then the corn oil (CO) was added. Pre-emulsions were then formed by pre-homogenization with a mixer (Oster Model 2612) for 2 minutes (González *et al*., 2007; Villalobos *et al*., 2017). Two ratios GA:CO [5:1 and 1:1] were used. The ratio 5:1 was used based on the low interfacial activity of GA so that must be used at much higher concentrations than other types of emulsifier commonly used to stabilize emulsions as reported by Huang *et al*. (2001). Also, there are works that reported high wall to core material ratios such as those by Beristain *et al*. (2001) who used ratios of mesquite gum:Cardamon oil of 5:1,4:1, 3:1, Zhao *et al*. (2017) who prepared emulsions of soybean oil with kudzu starch by using 5-30% (w/w) of soybean oil. All pre-emulsions were prepared at room temperature of 20 ± 1 °C.

2.3 Preparation of emulsions

The pre-emulsions were homogenized by using a LM10 microfluidizer (Microfluidics, England), as indicated by the D-optimal response surface design obtained with the Design Expert 11.0.5.0 software (Stat-Ease Inc., MN, USA). The categorical variable was the pressure used in the MF (69, 103 and 139 MPa) and the numerical variables were the ratios GA:CO. These pressures were selected based in works by Ricaurte *et al*. (2018) and Qiu, *et al*. (2015). All emulsions were processed by applying 2 microfluidization cycles (Granillo-Guerrero *et al*., 2017). To verify if experimental runs gave place to emulsions, Confocal Laser Scanning Microscopy images (Fig. 1) of the emulsions with the lowest stability (run 1), and three emulsions with an intermediate stability (runs 11, 12 and 24), were taken.

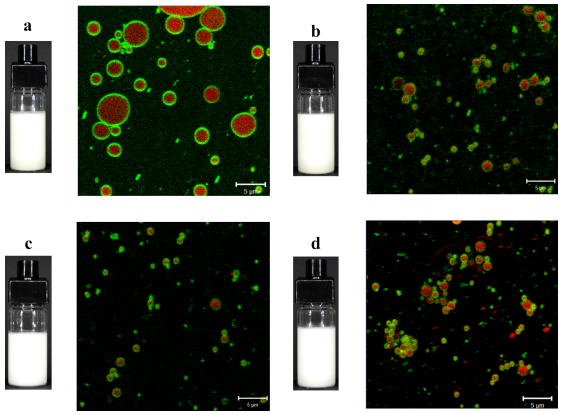

Fig. 1. CLSM images of emulsions and their macroscopic appearance corresponding to: a) run 1, b) run 11; c) run12 and d) run 24 (The dimensions of the tubes were, 27.5 x 70 mm).

Also, the emulsion 29 with the optimum stability is shown in Section 3.5, Fig. 8 and which was obtained by considering the minimum average droplet size (DS), polydispersity index (PDI) and Turbiscan® stability index (TSI) as response variables for a total of the 29 experimental runs (Table 1) in which the best emulsifying conditions which gave place to the optimum emulsion, according to the model were those for run 29 and are highlighted in a blue box in this Table. The models for DS, PDI and TSI are presented in Table 2 and were used to express the response variables as a function of the independent factor and its significant terms were found through analysis of variance (ANOVA).

The numerical optimization tool of the Design Expert software was used for the optimization of the response following the criterion of desirability (Ricaurte *et al*., 2018; Jeong and Kim, 2009). The response variables were fitted to models with R^2 values of 0.95, 0.98 and 0.96 for DS, PDI and TSI, respectively with a $p \leq 0.05$ and a non-significant lack-of-fit at $p > 0.05$. These results showed that the models were appropriate to predict the DS, PDI and TSI values for the emulsion used in this work (Table 3). A comparison of predicted and experimental DS, PDI and TSI values for the optimum emulsion, are presented in Table 4. The optimum emulsion was used to run all experiments aiming to investigate the characteristics of the emulsion before and after being atomized by the two nozzles described in the next section.

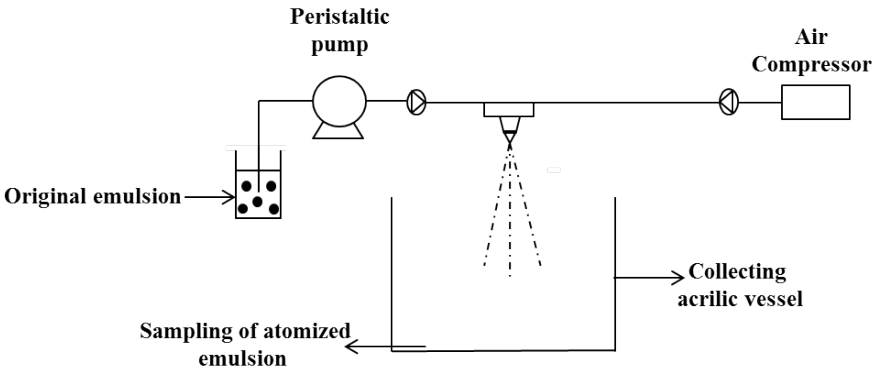

Fig. 2. Diagram of atomization experiment set-up.

2.4 Atomization of emulsions

A diagram of the experimental set up is shown in Fig. 2. Two different types of stainless steel two-fluid nozzles with external mixing were used to atomize the emulsion. The first one (NZ-1) was a model 48838 GEA-Niro (Denmark) and the second one (NZ-2) was a model JJ 1/8 SS Spraying Systems (EUA). NZ-1 had a 0.57 m long inner tube (0.006 m inside diameter) through which the fluid moved in the direction of a conical diameter reduction (60 degrees) for finally reaching the discharge orifice or slit (0.001 m inside diameter) in which fluid and air became into contact and produced the atomized mist (Fig. 3). The emulsion was fed at a rate of 1.14 L/h and the pressure of the atomizing air was 1kg/cm^2.

The second nozzle (NZ-2) had a short cylindrical (0.006 m height)-conical (50 degrees) conduct (0.003 m inside diameter) for the liquid which reaches the discharge orifice (0.0041 m inside diameter) in which air and fluid contact each other to atomize the liquid.

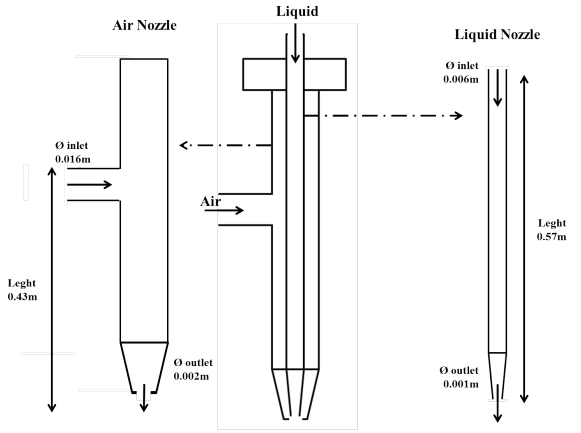

Fig. 3. Schematic representation of the nozzle NZ-1.

The emulsion was fed (as for NZ-1) at a rate of 1.14 L/h and the pressure of the atomizing air was, as for the NZ-1 nozzle, 1kg/cm^2. Geometry of NZ-2 nozzle forces liquid through a sudden change (90°) in its flow direction the air so increasing turbulence and wall-effects (Fig. 4).

In order to feed the emulsion to the nozzles, a peristaltic pump (Watson Marlow) having a range of rotational speeds of 1 to 200 rpm was used and to which a 0.5 m long tubing of silicone Cole-Parmer Instruments was fitted to transport the fed to the nozzles. The conduct had a wall of 0.159 cm and internal diameter of 0.478 cm. The atomized emulsion was collected at a distance of 30 cm from the nozzle (Munoz-Ibanez *et al*., 2015) in an acrylic vessel which was properly washed and dried between each experiment. Preliminary experiments showed that there were no effects of the pump and the plastic tubing on the DS and DS distribution which coincided with results by Munoz-Ibanez *et al*. (2015), when working with a nozzle and a disc atomizer.

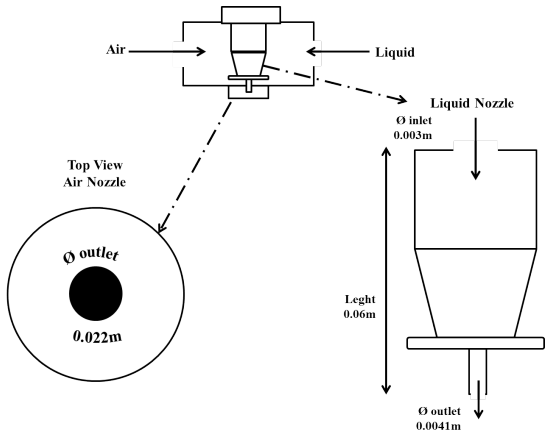

Fig. 4. Schematic representation of the nozzle NZ-2.

2.5 *Droplet size (DS) and polydispersity index (PDI)*

Average DS and PDI of prepared emulsions were evaluated by using a Zetasizer NanoZs (Malvern Instrument, England). All measurements were done by preparing a 1:1000 dilution (v/v) as reported by Garti *et al*. (1993), Huang *et al*. (2001) and Djordjevic *et al*. (2008) and a 1 mL sample of the diluted emulsion was placed into the measurement cell of the equipment (Mirhosseunni *et al*., 2008; Bernewitz *et al*., 2011). All measurements were carried out by triplicate.

2.6 *Determination of the stability of emulsion by the Turbiscan Stability Index (TSI)*

The stability of the emulsions was analyzed by using a Turbiscan® Lab. (Formulation Smart Scientific Analysis, France). Once the emulsions were prepared and atomized, a 20 mL sample was poured into a cylindrical glass cell and then, placed in the equipment for a 24h monitoring of the stability of the emulsion.

The TSI was taken as an indicator of the stability of the emulsions. This parameter embraces all phenomena that take place in the sample leading to destabilization (Qi *et al*., 2017) and considers variations detected in the samples in terms of size and/or concentration with time so that it allows to infer on the stability of the sample and to compare among different systems. The lower the TSI, the higher the emulsion stability so that values close to zero indicate greater stability in the emulsion (Kang *et al*., 2011). The TSI values were obtained by the software of the equipment by means of Eq. (1)

$$TSI = \sqrt{\frac{\sum_{i=1}^{n}(X_i - XBS)^2}{n-1}} \qquad (1)$$

in which: X_i is the average backscatter for each minute of the measurement, XBS is the mean of X_i and n is the number of scans.

2.7 *Ostwald ripening*

The fundamental theory of Ostwald ripening was established by Lifshitz and Slyozov and by Wagner (LSW theory) and is characterized by a constant volume rate (Wagner, 1961; Lifshitz and Slyozov, 1961), when the ripening is controlled by diffusion of the dispersed droplets across the continuous phase, and the cube of the radius of the average size droplet, increases linearly with time. To investigate the mechanism of destabilization of the original and atomized emulsions, the tendency to thermodynamic stability was associated to the change in the average droplet size as a function of time, following the methodology reported by Noor *et al*. (2013).

To determine if Ostwald ripening was contributing to the increment in size of emulsion droplets during time, samples of the emulsion were centrifuged at 500 x g at 20°C for 5, 10, 20, 30, 40, 50 and 60 min (Ricauter *et al*., 2018) and then, the average droplet size for each sample was determined as reported in Section 2.5. This method accelerates the ripening by centrifugation and describes the growing of particles that would happen at long destabilization times (Desplanques *et al*., 2012). The Oswald ripening parameter (ω) is described by Eq. (2):

$$\omega = \frac{d(r)^3}{d(t)} = \frac{8}{9}\left[\frac{Dc_\infty \gamma M}{\rho^2 RT}\right] \qquad (2)$$

Eq. 2, results from the application of the LSW theory to a single droplet into an infinite media in which the volume of the droplets increases with time due to the growth of large particles at the expense of the smaller ones (Gruner *et al*., 2016) and in which: r is the average radius of droplet, t is the storage time, M is the molar mass of dispersed phase (in our case of gum Arabic solution surrounding oil), ρ is the density of the continuous phase (solution of gum Arabic), c_∞ is the bulk solubility of the dispersed phase (in our case, of gum Arabic solutions), D is the diffusion coefficient of the droplets in the aqueous phase (in our case of droplets of gum Arabic surrounding oil into water), γ is the interfacial tension dispersed-dispersant (in our case, gum Arabic surrounding oil-gum Arabic solution). Interfacial tension increases and diffusion decreases with the radius of the particle and as ripening proceeds gradually larger particles (lower diffusion coefficient and larger interfacial tensions) will move towards the growing larger droplets which may possible cause the slope (ω) of the plot (r^3 vs t) to maintain a fairly constant value during ripening and its value represents the extent of the Ostwald ripening (Taylor *et al*., 1998). When the hydrophobic and hydrophilic groups of gum Arabic are oriented according to the affinity for the oil and aqueous phases, emulsion droplets change their diameter and their curvature angle.

Hydrophilic groups, on the other hand, are subjected to change their extent of attraction towards the dispersant thus of orientation of their polar groups towards such phase.

Table 1. D-optimal response surface experimental design for obtaining the optimum (working) emulsion (highlighted in blue box). Adjusted variables were: droplet size (DS), polydispersity index (PDI) and Turbiscan Stability index (TSI).

Run	Concentration of GA %(v/v)	Concentration of GA %(v/v)	Pressure (MPa)	Droplet size (nm)	PDI	TSI (at 24 h)
1	74.17	25.83	0	2232.15	0.961	8.09
2	88.11	11.89	0	2187.00	0.844	7.89
3	92.33	7.67	0	1847.50	0.908	7.15
4	92.33	7.67	0	1850.67	0.842	7.39
5	92.51	7.49	0	1833.00	0.876	7.07
6	16.50	6.06	0	2344.66	0.944	7.02
7	16.50	6.06	0	1684.46	0.944	6.17
8	94.52	5.48	0	1658.66	0.820	6.02
9	74.17	25.83	69	784.10	0.342	4.32
10	86.33	13.67	69	750.30	0.295	4.46
11	88.02	11.98	69	742.53	0.310	5.00
12	92.44	7.56	69	616.16	0.158	3.21
13	93.32	6.68	69	528.27	0.144	3.55
14	93.32	6.68	69	524.95	0.150	3.61
15	94.03	5.97	69	682.13	0.141	2.98
16	94.52	5.48	69	697.80	0.100	2.78
17	74.17	25.83	103	816.00	0.326	4.56
18	74.17	25.83	103	917.46	0.189	5.12
19	91.18	8.82	103	522.35	0.226	4.01
20	91.60	8.40	103	599.60	0.122	3.41
21	91.60	8.40	103	568.70	0.137	2.48
22	92.63	7.37	103	549.77	0.177	2.34
23	94.52	5.48	103	579.65	0.112	2.25
24	74.17	25.83	139	906.90	0.309	1.88
25	88.18	11.82	139	822.90	0.384	1.43
26	91.60	8.40	139	625.15	0.286	1.45
27	91.60	8.40	139	624.13	0.207	1.69
28	93.96	6.04	139	619.05	0.151	1.55
29	94.52	5.48	139	585.99	0.129	1.16

Given this situation, the fitting of r^3 vs t would produce a slope equivalent to a coefficient which considers all the above phenomena and which magnitude has been named as the Ostwald ripening parameter (Taylor, 1998; Santos *et al*., 2017).

2.8 *Confocal Scanning Laser Microscopy of emulsions*

Confocal Scanning Laser Microscopy (CSLM) was performed by using a LSM 710 NLO microscope (Carl Zeiss, Germany). The lipid phase of the emulsions were dyed using a 0.1% solution of Nile red (Sigma Co., USA). The wall material (GA) was dyed with a 0.05% solution of FITC (Fluorescein Isothiocyanate, Sigma Co., USA) which was added to the sample and allowed to stand for 5 minutes. Then, 0.5 μL of the prepared sample were mounted on glass slides and observed under the CLSM at a laser wavelength of 488 nm (Nile red) and 514 nm (FITC) with. The images were taken with a 63X/1.40 plan-apochromat oil DIC M27 objective at a resolution of 512×512 pixels (size of pixel was $0.19\mu m^2$). Thickness of the wall material of the droplets was evaluated by using the ImageJ software (National Institutes for Health, Bethesda, USA).

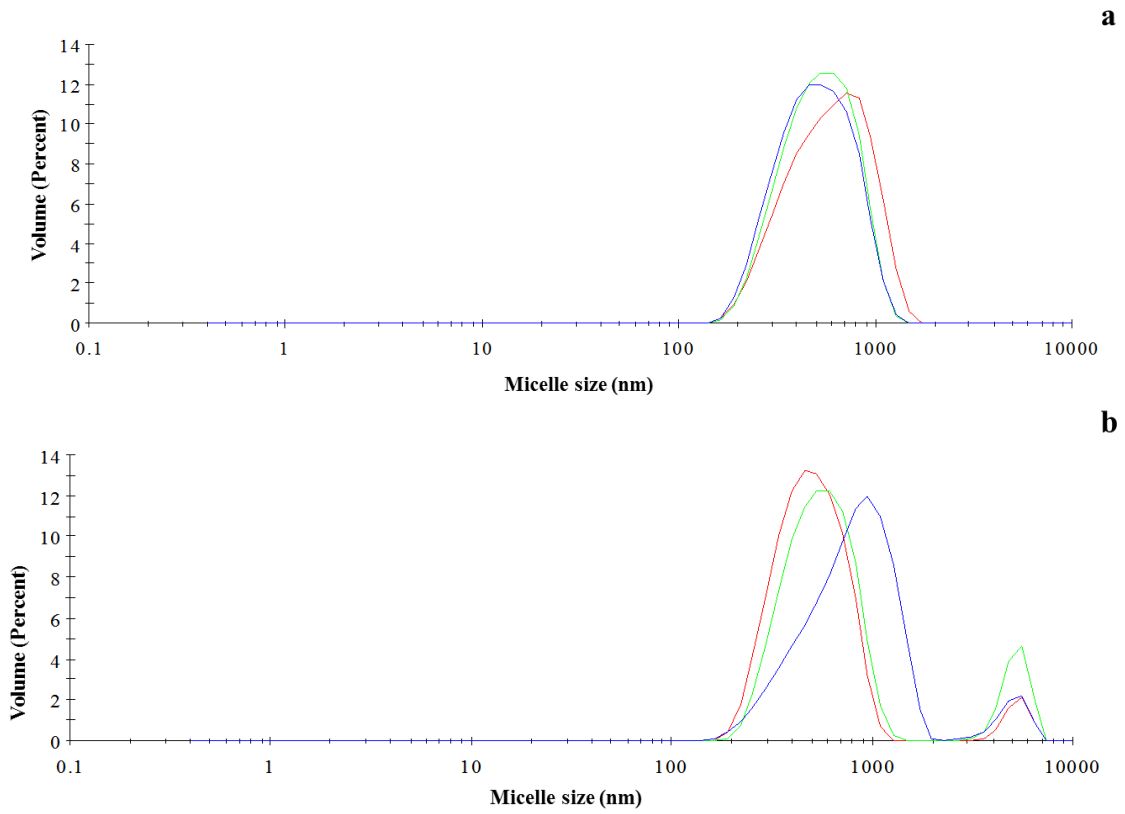

Fig. 5. Droplet size distribution of original emulsion (green) and NZ-1 (red) and NZ-2 (blue) atomized emulsions; a, original emulsions and b, emulsions after 24 h.

2.9 Statistical analysis

As mentioned above (Section 2.2.2), the optimum emulsion was obtained by using the D-optimal response surface design methodology in the Design Expert Version 11.0.5.0 software (Stat-Ease Inc., MN, USA). To evaluate the differences between the properties of the emulsions before and after being atomized, to all results, an analysis of variance (ANOVA) was applied by using the statistical software MyStat 12 (Statistical Software Package, SisTat, USA). The significance level was considered at $p \leq 0.05$. The mean ± standard deviations were reported in every case.

3 Results and discussion

3.1 Formulation of the optimum emulsion

The emulsions were evaluated for minimum DS, PDI and TSI as mentioned in Section 2.3 and optimum formulation (run 29 of the experimental design in Table 1) was composed of an oil phase (4.76% w/w); gum Arabic solution (25% w/w) and was produced when microfluidizer pressure was 139 MPa and by using 2 microfluidization cycles.

3.2 Influence of the atomization devices on DS and PDI

Preparation of pre-emulsions induce non-polar groups to form large droplets thus reducing the contact surface with water molecules so generating an important contribution to the free energy of the system (Tu *et al.*, 2013). These droplets were further divided into smaller drops in the microfluidizer.

Results in Table 1 showed that the pre-emulsion feed to the microfluidizer had an average DS = 1658.7 nm and a PDI = 0.82 which were further reduced to 591.0 nm and 0.13 respectively in the microfluidizer.

Table 2. ANOVA for the adjusted variables to response optimization design: DS, PDI and TSI for the oil in water emulsions homogenizer by microfluidizer.

Factor	DS(nm)			Factor	PDI			Factor	TSI		
	Sum of squares	df	p-Value		Sum of squares	df	p-Value		Sum of squares	df	p-Value
Model	1.00E+07	8	< 0.0001	**Model**	2.83	7	< 0.0001	**Model**	128.46	7	< 0.0001
A-A	2.80E+05	1	0.0008	A-A	0.0907	1	< 0.0001	A-A	10.44	1	< 0.0001
B-B	9.91E+06	3	< 0.0001	B-B	2.8	3	< 0.0001	B-B	122.39	3	< 0.0001
AB	41150.89	3	0.5238	AB	0.0253	3	0.0298	AB	2.16	3	0.0194
A^2	1.10E+05	1	0.0219								
Residual	3.56E+05	20		**Residual**	0.0488	21		**Residual**	3.68	21	
Lack of Fit	1.32E+05	14	0.9839	Lack of Fit	0.0341	15	0.5844	Lack of Fit	2.67	15	0.5039
Pure Error	2.24E+05	6		Pure Error	0.0148	6		Pure Error	1	6	
Cor Total	1.04E+07	28		**Cor Total**	2.88	28		**Cor Total**	132.14	28	
R-Squared	0.9656			**R-Squared**	0.9830			**R-Squared**	0.9722		
Adj R-Squared	0.9519			**Adj R-Squared**	0.9774			**Adj R-Squared**	0.9629		

Upon atomization a different phenomenon was observed (see below) since the wall material layers around oil droplets were reduced in thickness so exposing polar groups towards the outside which destabilizes the system. The emulsion that was atomized by means of NZ-1 did not show significant difference in droplet size ($p > 0.05$) with respect to the original emulsion at time zero (just after preparation), whereas the emulsion that was atomized by using the NZ-2 presented a significant ($p \leq 0.05$) increment (10.60%) in droplet size with respect to the original emulsion (Table 5). Droplet size is one of the most important factors affecting the dynamic stability of emulsions and its disruption is, strongly dependent on the energy input during handling/processing (Floury *et al*., 2002 and 2004; Kolb *et al*., 2001; Perrier-Cornet *et al*., 2005). Calculated (Table 6) difference in velocities air-liquid were: 59.30 and 267.55 m/s for NZ-1 and NZ-2 respectively, so producing larger collision effects between these two streams of fluids and therefore larger shear when atomizing through NZ-2.

Differences in shear stresses caused by the components of the nozzles, which due to their geometric configuration increase and reduce flow diameters and suffer a sudden decrease in fluid pressure when leaving the nozzles and had (NZ-2) a sudden (90°) change of liquid flow direction (Section 2.4), gave place to a thermodynamically more unstable emulsion as compared to the original one by reducing the wall material layer (as was probed by CLSM images, Section 3.5) and by exposing non polar groups towards the gum-water interphase.

Also, the electrostatic interactions of charged polysaccharides on the surfaces of opposite charge biopolymers such as gum Arabic destabilized the wall material layer (Guzey, 2007; Harnsilawat *et al*., 2006) and could be influenced by the stress caused by the nozzles by changing the distribution of the polar-non-polar groups ratio of the gum in addition to forming new surfaces. All the above, affected the DS (NZ-2) and PDI (for both nozzles) of the atomized emulsions as described and had an effect on the other stability-related parameters studied (see Sections 3.3-3.5 below).

After 24 hours of atomization, the emulsions passed by the two nozzles presented significant increase of DS ($p \leq 0.05$) with respect to the original emulsion. (16.89% in DS for the emulsion atomized by NZ-2 and a 9.68% for the NZ-1) (Table 5). Significant differences ($p \leq 0.05$) were observed in the PDI's values for the original and the two atomized emulsions. NZ-1 and NZ-2 atomized emulsion, presented an increase of 21.88% and 38.28% respectively with respect to the original emulsion (Fig. 5). Significant differences ($p \leq 0.05$) were observed in the PDI's values for the original and the two atomized emulsions. NZ-1 and NZ-2 atomized emulsion, presented an increase of 21.88% and 38.28% respectively with respect to the original emulsion (Fig. 5).

The shear rate applied during atomization influences the size and distribution of the droplet in the emulsions used for different applications such as spray drying, electro spraying, vibrating-jet- encapsulation, film formation, coating and others (Kanellopoulos *et al*., 2017; Haffner *et al*., 2016; Wais *et al*., 2016). Once more, it is stressed that, the characteristics of these final products should be related to those of the atomized emulsion, according to results obtained.

3.3 Turbiscan Lab® stability index (TSI)

Turbiscan Stability indexes obtained, indicated that, the original emulsion had a greater stability after the first 2 hours with respect to atomized ones.

Table 3. Equations for DS, PDI and TSI for the oil in water emulsions homogenizer by microfluidizer.

Droplet size (nm)	$DS = 916.99 - 139.08(A) + 996.19(B) - 332.36(B) - 362.36(B)$ $-59.94(A)(B) + 81.98(A)(B) - 6.07(A)(B) + 153.03(A)^2$
Polydispersity Index	$PDI = 0.3775 - 0.0804(A) + 0.5164(B) - 0.1705(B) - 0.2089(B)$ $+0.0686(A)(B) - 0.0371(A)(B) + 0.0026(A)(B)$
Turibiscan stability index	$TSI = 3.91 - 0.8853(A) + 3.31(B) - 0.1598(B) - 0.7492(B)$ $-0.0896(A)(B) - 0.0174(A)(B) - 0.5482(A)(B)$

This agrees with results obtained for the DS and PDI (See Section 2.2 above) given that smaller droplets have been associated to higher stability (McClements, 1999). Within the first two hours the three emulsions did not present significant differences ($p > 0.05$) in TSI values. It was observed that, as from three hours, the stability of the two atomized emulsions started having significant changes ($p \leq 0.05$) in this parameter, being 52.50 and 97.50% (NZ-1 and NZ-2 respectively) more unstable (higher TSI's) with respect to the original one (not atomized) (Fig. 6). Protein fractions of gum Arabic helped to stabilize the emulsions since they tend to adsorb on the oil-water interface.

Obtained decrements in stability of the droplets due to atomization could be due to rearrangements of the hydrophobic groups associated to the protein fraction which, for the atomized emulsions, decreased emulsifying capacity of gum Arabic (Villalobos-Castillejos *et al*., 2017). Electrostatic forces derived from shear could also be affected during atomization and may also influence the stability of the emulsions. Mirhosseini (2008) reported that in emulsions with orange oil and different amounts of gum Arabic, the stability was affected by the amount of GA which also affected electrical conductivity of the dispersion.

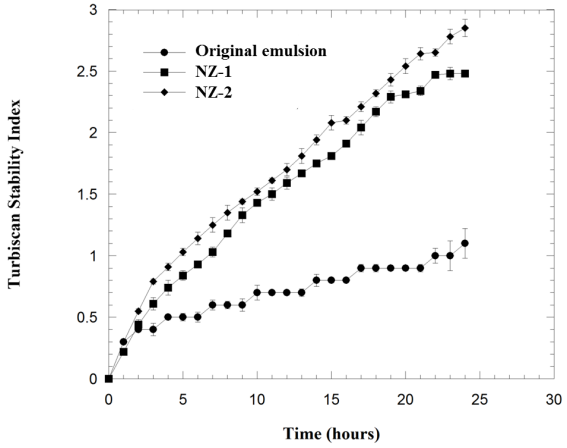

Fig. 6. Turbiscan Stability Index for the three emulsions.

The high shear rates applied to the emulsions when passing through the nozzles, which were of different extent due do the inherent design of the two nozzles (Sections 2.4 and 3.2 above) caused differences in steric and electrostatic alterations to the system which, in addition to the decrease of wall material observed in CLSM images (Section 3.5 below), increased the instability of the formed droplets by creating new surfaces which gives place to the formation of overall new emulsions whose ripening and flocculation kinetics caused the increment of TSI during the 24 h of measurements.

Given that the presence of gum Arabic provided a better long-term stability, by immobilizing the emulsion droplets into a network stabilized by electrostatic repulsions or steric effects between the droplets (Dickson, 2009), the observed decrements of the thicknesses of droplets due to differences in shear during atomization with both nozzles (NZ-2 having more tortuous liquid path and smaller outlet slit) provoked destabilization with time.

3.4 Destabilization mechanism of emulsion by Ostwald ripening

Ostwald ripening is the process in which larger droplets grow at the expense of smaller ones which move through the continuous phase reaching larger droplets (Kabalnov *et al*., 1992; Weis *et al*., 2001; Chanamai *et al*., 2002).

Table 4. Comparison of values predicted by the design (with a Desirability of 0.965) and the ones obtained experimental with the corresponding percentage of error.

Point	Experimental	Predicted	% of error
DS	591.99±6.42	613.54	3.51
IPD	0.128±0.004	0.126	1.56
TSI	1.16±0.05	1.282	9.51

Table 5. Velocities of air and emulsions at the outlet slits of the nozzles.

Nozzle	Velocity of the liquid at the outlet of nozzle (m/s)	Velocity of the air at the outlet of nozzle (m/s)
NZ-1	0.40	59.70
NZ-2	2.44	269.99

These findings indicated that the forces that mainly controlled the destabilization of emulsions responded to an Ostwald ripening mechanism. Joye *et al*. (2014) and Ricaurte *et al*. (2018), reported that the Ostwald ripening destabilization was more pronounced for emulsions having smaller droplet sizes because these emulsions are, thermodynamically, more unstable due to Brownian motion associated to smaller droplets and which is, consequently, more pronounced than for larger ones. Obtained values of the slope (r^3 vs t) were similar to those reported by Ricaurte *et al*. (2018). Variation of droplet radius with time due to diffusion of small molecules towards larger ones (Ostwald ripening) was probed by the good-fit ($R^2 \geq 0.98$) of the r^3 vs t straight lines as described in Section 2 (Fig. 7). Slopes (ω) of the straight lines obtained were: $\omega = 1.60 \times 10^{-24}$ m^3/s (for original emulsion); $\omega = 1.08 \times 10^{-23}$ m^3/s (for emulsion atomized by NZ-1 nozzle) and $\omega = 1.25 \times 10^{-23}$ m^3/s (for emulsion atomized by NZ-2 nozzle) indicating that the magnitude of the Ostwald ripening phenomena with time was in the following order: NZ-2>NZ-1>Original emulsion, and agrees with destabilization indicators obtained for DS, PDI, TSI described in Sections 3.2 and 3.3.

Also, the thicknesses of the wall material for original and atomized emulsions were larger for the original emulsion than for NZ-1 and NZ-2 atomized emulsions and these decrements with respect to the original emulsion which were larger for NZ-2 than for NZ-1 as described in Section 3.5 on CLSM images of the emulsions.

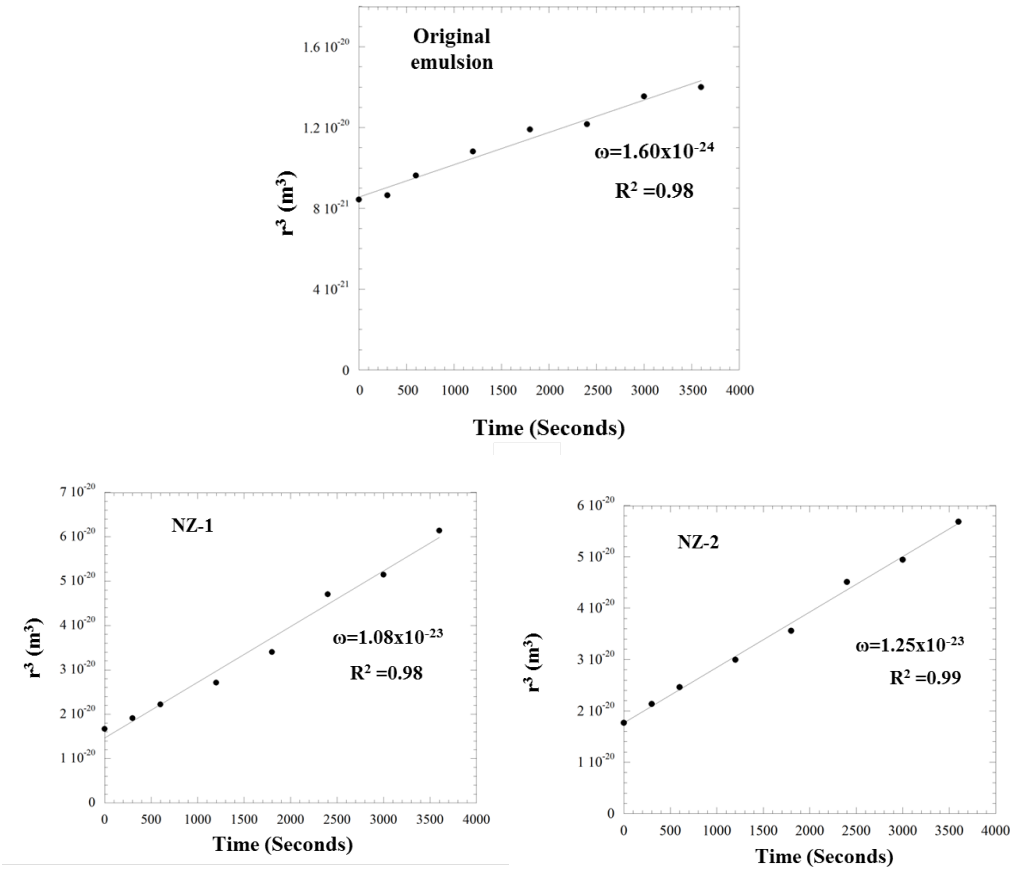

Fig. 7. Ostwald ripening plots: the cube of the droplet radius (r^3) as a function of time for the original emulsion; NZ-1 and NZ-2.

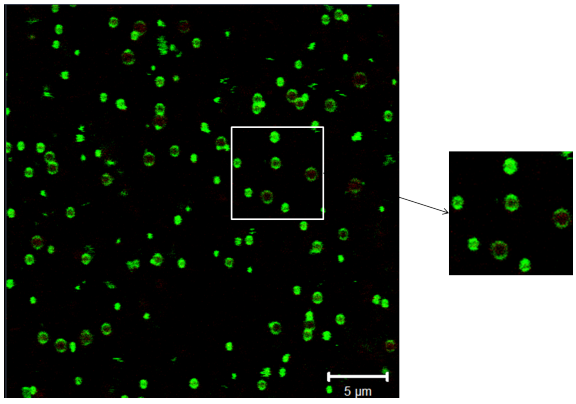

Fig. 8. Images of CLSM of emulsion prepared by microfluidization.

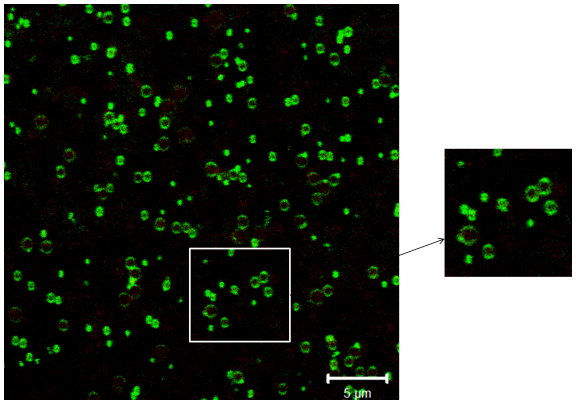

Fig. 9. Images of CLSM of emulsion homogenizer by NZ-1 after atomization.

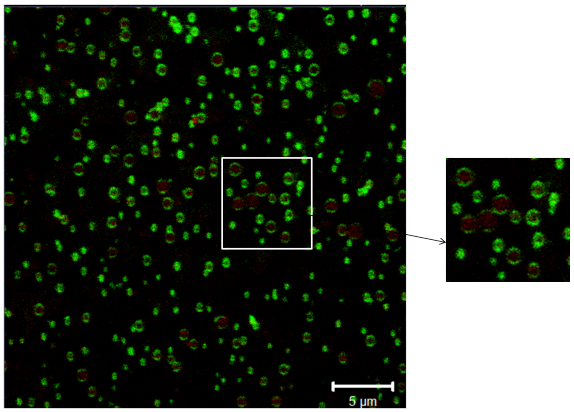

Fig. 10. Images of CLSM of emulsion homogenizer by NZ-2 after atomization.

The interfacial tension of an oil in water interface increases with size of droplet which in our case caused larger values of the slope of the straight lines mentioned above for atomized emulsions. The mean droplet volume as indicated by the r^3 value for the original emulsion increased up to 1.18 times with respect to its initial value after 60 min of centrifugation, while for the emulsions atomized by the NZ-1 and NZ-2 nozzles, increments in r^3 were 1.47 and 1.54 times their initial values after the same time. These results are an indicator of the speed of increase of DS and agreed with those found by the evaluation of the TSI as discussed in Section 3.3.

3.5 Confocal laser scanning microscopy (CLSM) of emulsions

CLSM images of original (Fig. 8) and atomized emulsions (Figs. 9 and 10) showed that the droplets were properly formed with wall material (green) covering the oil phase (red). However, it was possible to observe a decreased thickness of the wall material (green area in Figs. 9 and 10) (as % of green area respect to the original emulsion) surrounding the oil phase.

Decrements of coverage were: 29.87 and 49.98% for emulsions atomized by using NZ-1 and NZ-2 respectively. Such decrements may be the cause of the loss of stability with time for atomized emulsions as discussed in sections 3.1-3.3 above. It has been reported that the microstructure of the emulsion, has an influence on the efficiency of encapsulation since it influences the release and viability of the active ingredient of capsules obtained by spray drying (McClements and Rao 2011; McClements and Li, 2010). Fernandez *et al*. (2005) when studying two oils (tributyrin and triolein) in oil concentration varying from 1 to 5% (v/v) emulsions stabilized with gum Arabic, the coating of the droplets was properly formed and stated that the formation of a thick layer of wall material helps to achieving such protection. Our results confirmed that he nozzle produced a different emulsion than the original emulsion, not only due to a thinner layer of wall material but also in their charge-related characteristics which produced the overall consequence of destabilizing the emulsions. It is important to mention that the decrement in thickness of the wall material exposes (in the first instance) non-polar groups to the continuous phase which causes rearrangements of polar-non polar groups thus provoking destabilization of droplets and of the entire system and these systems will tend to ripen. This disruption of droplets highlights the need to characterize the final product (capsules, films, coatings, etc.) based mainly on the properties of the actual atomized emulsion.

Table 6. Droplet size (DS) and polydispersity index (PDI) of original and atomized emulsions at time zero and after 24h.

Sample	DS (nm) time zero	PDI time zero	DS (nm) (24 hours)	PDI (24 hours)
Original emulsion	591.99±6.42^a	0.128±0.004^a	614.37±12.05^a	0.134±0.004^a
NZ-1	613.00±11.15^a	0.156±0.005^b	695.77±6.00b^b	0.245±0.004^b
NZ-2	654.74±12.91^b	0.177±0.003^c	765.39±10.59^c	0.287±0.002^c

Different letters in superscripts in the same colum, indicate significant difference.

Conclusions

Cumulative evidence from the various experiments carried out, as well theoretical and experimental research described in the different sections of this work, indicated that the two atomization devices used under nominal operating conditions, produced the destabilization of the droplets prepared by microfludization which could be due to the high shear given to the emulsions by such devices as indicated by changes of DS, PDI and TSI (of both atomized emulsions) in respect to the original emulsion. These changes were due to the thinning of the wall material layer produced during passage through the nozzles and the concomitant exposure of new surfaces to the media which included non-polar groups so decreasing the entropy of the system. It was observed that stability parameters changed more pronouncedly for NZ-2 atomized emulsion sine this nozzle had the larger differential liquid-air velocity (larger drag) at the outlet and its configuration caused a sudden change (90°) in the direction of the liquid before encountering the air. On the other hand, NZ-1 had a much larger diameter of the liquid conduct as compared to NZ-2 which decreased shear-wall and the liquid enters axially to the outlet orifice (no sudden change in direction). Original and atomized emulsions were destabilized differently by Ostwald ripening and its magnitude was larger for atomized emulsions, probably due to compensation of interfacial-diffusional effects. During the time the emulsions were tested for DS, PDI and TSI, destabilization was mainly due to polar groups exposed to the media. CLSM images confirmed the decrease in thickness of the droplets which strongly influenced the destabilization of emulsions due to the abovementioned charge disruption. Finally, it is recommended to correlate the properties of the final end product (capsules, films, coatings, etc.) not only with those of the original microfluidized emulsions but also with those of the atomized emulsions, by including during the preparation by atomization of films, coatings, capsules, etc., a proper selection of the atomizer and a sampling-characterization on-line scheme.

Acknowledgements

The first author is grateful for the support to the Consejo Nacional de Ciencia y Tecnología (CONACYT) and IPN in the form of study grants to pursue her PhD degree in Food Science within the doctoral program of the Instituto Politécnico Nacional, included in the Postgraduate Registry of Programs. Authors thank CONACYT and IPN for financial support to carry out the investigation and University of La Sabana, in Chia, Colombia for extensive collaboration with atomization experiments

References

Aliseda, A., Hopfinger, E.J., Lasheras, J.C., Kremer, D.M., Berchielli, A., Connolly, E.K. (2008). Atomization of viscous and non-Newtonian liquids by a coaxial, high-speed gas jet. Experiments and droplet size modeling. *International Journal of Multiphase Flow 34*, 161-175. DOI: https://doi.org/10.1016/j.ijmultiphaseflow.2007.09.003

Beristain, C.I.,García, H.S., Vernon-Carter, E.J. (2001). Spray-dried encapsulation of cardamom (*Elettaria cardomomum*) essential oil with mesquite (*Prosopis juliflora*) gum. *LWT-Food Science and Technology 34*, 398-401.

Bernewitz, R., Guthausen, G., Schuchmann, H.P. (2011). NMR on emulsions: characterization

of liquid dispersed systems. *Magnetic Resonance in Chemistry 49*, 93-104. DOI: https://doi.org/10.1002/mrc.2825

Chanamai, R., Horn, G., McClement, D.J. (2002). Influence of oil polarity on droplet growth in oil-in-water emulsions stabilized by a weakly adsorbing biopolymer or a nonionic surfactant. *Journal of Colloid and Interface Science 247*, 167-176. DOI: 10.1006/jcis.2001.8110

Desplanques, S., Renou, F., Grisel, M., Malhiac, C. (2012). Impact of chemical composition of Xanthan and acacia gums on the emulsification and stability of oil-in-water emulsions. *Food Hydrocolloids 27*, 401-410. DOI: https://doi.org/10.1016/j.foodhyd.2011.10.015

Dickinson, E. (2009). Hydrocolloids as emulsifiers and emulsion stabilizers. *Food Hydrocolloids 23*, 1473-1482. DOI: https://doi.org/10.1016/j.foodhyd.2008.08.005

Djorjevic, D., Cercaci, L., Alamed, J., McClements, D.J., Decker, E.A. (2008). Chemical and physical stability of proyein and gum arabic-stabilized oil-in-water emulsions conatining limonene. *Journal of Food Science 73*, 167-172. DOI: https://doi.org/10.1111/j.1750-3841.2007.00659.x

Fernández-Arteaga, A. (2006). Preparación, caracterización y estabilidad de emulsiones y microemulsiones O/W. Tesis doctoral en Alimentos. Universidad de Granada, España.

Floury, J., Belletre, J., Legrand, J., Desrumaux, A. (2004a). Analysis of a new type of high pressure homogenizer. A study of the flow pattern. *Chemical Engineering Science 59*, 843-853. DOI: https://doi.org/10.1016/j.ces.2003.11.017

Floury, J., Desrumaux, A., Axelos, M.A.V., Legend, J. (2002). Degradation of methylcellulose during ultra-high pressure homogenization. *Food Hydrocolloids 16*, 47-53. DOI: https://doi.org/10.1016/S0268-005X(01)00039-X

Foerster, M., Gengenbach, T., Woo, M.W., Selomulya, C. (2016). The impact of atomization on the surface composition of spray-dried milk droplets. *Colloids and surface B: Biointerfaces 149*, 460-471. DOI: http://dx.doi.org/10.1016/j.colsurfb.2016.01.012

Fuentes-Ortega, F., Marínez-Vargas, S.L., Cortés-Camargo, S., Guadarrama-Lezama, A.Y., Gallardo-Rivera, R., Baeza-Jimenéz, R., Pérez-Alonso, C. (2017). Effects of the process variables of microencapsulation sesame oil (*Sesamum indica* L.) by spray drying. *Revista Mexicana de Ingeniería Química 16*, 477-490.

Garti, N., Lesser, M.E. (2001). Emulsification properties of hydrocolloids. *Polymers for advanced Technologies 12*, 123-135. DOI: https://doi.org/10.1002/1099-1581(200101/02)12:1/2<123::AID-PAT105>3.0.CO;2-0

González-Rodríguez, M.L., Barros, L.B., Palma, J., González-Rodríguez, P.L., Tabasco, A. M. (2007). Application of statical experimental design to study the formulation variables influencing the coating process of lidocaine liposomes. *International Journal of Pharmaceutics 337*, 336 - 345. DOI: http://dx.doi.org/10.1016/j.ijpharm.2007.01.024

Granillo-Guerrero, V.G., Villalobos-Espinosa, J.C., Alamilla-Beltrán, L., Téllez-Medina, D.I., Hernández-Sánchez, H., Dorantes-Álvarez, L., and Gutiérrez-López, G.F. (2017). Optimization of the formulation of emulsions prepared with a mixture of vitamins D and E by means of an experimental design simplex centroid and analysis of colocalization of its components. *Revista Mexicana de Ingeniería Química 16*, 816-872.

Gruner, P., Riechers, B., Semin, B., Lim, J., Johnston, A., Short, K., Baret, J.C. (2016). Controlling molecular transport in minimal emulsions. *Nature Communications*. DOI: 10.1038/ncomms10392

Guzey D, McClements DJ. (2007). Impact of electrostatic interactions on formation and stability of emulsions containing oil droplets coated by β-lactoglobulin-pectin complexes. *Journal of Agricultural and Food Chemistry 55*, 475-85. DOI: 10.1021/jf062342f

Haffner, F.B., Diab, R., Pasc, A. (2016). Encapsulation of probiotics: insights into academic and industrial approaches.*AIMS Materials Science 3*, 114-136. DOI: 10.3934/matersci.2016.1.114

Hakansson A., Rayner M. (2018) General principles of nanoemulsion formation by high-energy mechanical methods. *Nanoemulsions 5*, 104-139. DOI: https://doi.org/10.1016/B978-0-12-811838-2.00005-9

Harnsilawat, Pongsawatmanit, R., McClements, D. J. (2006). Stabilization of model beverage cloud emulsions using protein-polysaccharide electrostatic complexes formed at the oil-water interface. *Journal of Agricultural and Food Chemistry 54*, 5540-5547. DOI: 10.1021/jf052860a

Hede, P.D., Bach, P., Jensen, A.D. (2008). Two-fluid spray atomization and pneumatic nozzle for fluid bed coating/agglomeration purpose: a review. *Chemical Engineering Science 63*, 3821-3842. DOI: https://doi.org/10.1016/j.ces.2008.04.014

Huang, X., Kakuda, Y., Cui, W. (2001). Hydrocolloids in emulsions: particle size distribution and interfacial activity. *Food Hydrocolloids 15*, 522-542. DOI: https://doi.org/10.1016/S0268-005X(01)00091-1

Jafari SM, He Y., Bhandari B. (2007). Effectiveness of encapsulating biopolymers to produce submicron emulsions by high energy emulsification techniques. *Food Research International 40*, 862-873. DOI: https://doi.org/10.1016/j.foodres.2007.02.002

Jafari. SM., He Y., Bhandari B. (2007). Production of sub-micron emulsions by ultrasound and microfluidization techniques. *Journal of Food Engineering 82*, 478-488. DOI: https://doi.org/10.1016/j.jfoodeng.2007.03.007

Jeong, I.-J., & Kim, K.-J. (2009). An interactive desirability function method to multi-response optimization. *European Journal of Operational Research 195*, 412-426. DOI: http://dx.doi.org/10.1016/j.ejor.2008.02.018.

Joye, I.J., Davidov-Pardo, G., McClements, D.J. (2014). Nanotechnology for increased micronutrient bioavailability. *Trends in Food Science and Technology 40*, 168-182. DOI: https://doi.org/10.1016/j.tifs.2014.08.006

Kabalnov, A., Shchukin, E. (1992). Ostwald ripening theory: applications to fluorocarbon emulsion stability. *Advances in Colloid and Interface Science 38*, 69-97. DOI: https://doi.org/10.1016/0001-8686(92)80043-W

Kanellopoulos, A., Giannaros, P., Palmer, D., Kerr, A., Al-Tabba, A. (2017). Polymeric microcapsules with switchable mechanical properties for self-healing concrete: Synthesis, characterization and proof of concept. *Smart Materials and Structures 26*, 045025. DOI: https://doi.org/10.1088/1361-665X/aa516c

Kang, W., Xu, B., Wang, Y., Li, Y., Shan, X., An, F., & Liu, J. (2011). Stability mechanism of W/O crude oil emulsion stabilized by polymer and surfactant. *Colloids and Surfaces A: Physicochemical and Engineering Aspects 384*, 555-560. DOI: https://doi.org/10.1016/j.colsurfa.2011.05.017

Kolb, G., Viardot, K., Wagner, G., Ulrich, J. (2001). Evaluation of a new high-pressure dispersion unit (HPN) for emulsification. *Chemical Engineering and Technology 24*, 293-296. DOI: https://doi.org/10.1002/1521-4125(200103)24:3<293::AID-CEAT293>3.0.CO;2-0

Lifshitz, I.M., Slyozov, V.V. (1961). The kinetics of precipitation from supersaturated solid solutions. *Journal of Physical and Chemistry of Solids 19*, 35-50. DOI: 10.1016/0022-3697(61)90054-3

McClements, D.J. (1999). *Food Emulsions: Principles, Practice and Techniques*. CRC Press LLC, USA.

McClements, D.J. (2007). Critical review of techniques and methodologies for characterization of emulsion stability. *Critical Reviews in Food Science and Nutrition 47*, 611-649. DOI: https://doi.org/10.1080/10408390701289292.

McClements, D.J. (2015). *Food Emulsion: Principles, Practice and Techniques*. Third Edition. CRC Press Taylor, USA.

McClements, D.J., Jafari S.M. (2018). General aspects of nanoemulsions and their formulation. In: *Nanoemulsions formulation, applications, and characterization* (McClements, D.J. and Jafari eds.), Pp. 3-17. U.S.A. DOI:

https://doi.org/10.1016/B978-0-12-811838-2.00 001-1

McClements, D.J., Li, Y. (2010). Structured emulsion-based delivery systems: controlling the digestion and release of lipophilic food components. *Advances in Colloid and Interface Science 159*, 213-228. DOI: https://doi.org/10.1016/j.cis.2010.06.010

McClements, D.J., Rao, J. (2011). Food-grade nanoemulsions: Formulation, fabrication, properties, performance, biological fate, and potential toxicity. *Reviews in Food Science and Nutrition 51*, 285-330. DOI: http://dx.doi.org/10.1080/10408398.2011.559558.

Mirhosseini, H., Tan, C.P., Hamid, N., Yusof, S. (2008). Effect of Arabic gum, xanthan gum and orange oil content on potential, conductivity, stability, size index and pH of orange beverage emulsion. *Colloids and Surfaces A 315*, 7-56. DOI: http://dx.doi.org/10.1016/j.colsurfa.2007.07.007.

Munoz-Ibanez, M., Azagoh, C., Dubey, B. N., Dumoulin, E., Turchiuli, C. (2015). Changes in oil-in-water emulsion size distribution during the atomization step in spray-drying encapsulation. *Journal of Food Engineering 167*, 122-132. DOI: http://dx.doi.org/10.1016/j.jfoodeng.2015.02.008.

Noor El-Din, M. R., El-Hamouly, S. H., Mohamed, H. M., Mishrif, M. R., Ragab, A. M. (2013). Water-in-diesel fuel nanoemulsions: Preparation, stability and physical properties. *Egyptian Journal of Petroleum 22*, 517-530. DOI: http://dx.doi.org/10. 1016/j.ejpe.2013.11.006.

Ogawa, S., Decker, E.A., McClements, D.J. (2003). Production and characterization of O/W emulsions containing cationic droplets stabilized by lecithin-chitosan membranes. *Journal of Agricultural and Food Chemistry 51*, 2806-2812. DOI: 10.1021/jf020590f.

Perrier-Cornet, J.M., Marie, P. and Gervais, P. (2005). Comparison of emulsification efficiency of protein-stabilized oil-in-water emulsions using jet, high pressure and colloid mill homogenization. *Journal of Food Engineering 66*, 211-217. DOI: https://doi.org/10.1016/j.jfoodeng.2004.03.008

Qi. X., Dond, Y., Wang, H., Wang C., Li F. (2017). Application of Turbiscan in the homoaggregation and heteroaggregation of copper nanoparticles. *Colloids and Surfaces A 535*, 96-104. DOI: https://doi.org/10.1016/j.colsurfa.2017.09.015

Ricaurte, L., Hernández-Carrión, M., Moyano-Molano, M., Clavijo-Romero, A., Quintanilla-Carvajal., M.X. (2018). Physical, thermal and thermodynamical study of high oleic palm oil nanoemulsions. *Food Chemistry 256*, 62-70. https://doi.org/10.1016/j.foodchem.2018.02.102.

Santos, J., Calero, N., Trujillo-Cayado, L.A., Garcia, M.C., Muñoz, J. (2017). Assessing differences between Ostwald ripening and coalescence by rheology, laser diffraction and multiple light scattering. *Colloids and surfaces B: Biointerfaces 159*, 405-411. DOI: http://dx.doi.org/10.1016/j.colsurfb.2017.08.015

Tadros, T., Izquierdo, R., Esquena, J., Solans, C. (2004). Formation and stability of nano-emulsions. *Advances in Colloid and Interface Science*, 108-109:303-318. DOI: https://doi.org/10.1016/j.cis.2003.10.023.

Tadros, T.F. (2013). Emulsion formation and stability. In: *Emulsion Formation, Stability, and Rheology*, (eds.), Pp. 1-75. (NY). DOI: https://doi.org./10.1002/9783527647941.ch1.

Taherian, A.R., Fustier, P., Ramswamy, H.S. Steady and dynamic shear rheological properties, and stability of non-flocculated and flocculated beverage cloud emulsions. *International Journal of Food Properties 11*, 24-43. DOI: 10.1080/10942910601171978

Taylor, P. (1998). Ostwald ripening in emulsions. *Advances in Colloid and Interface Science 75*, 107-163. DOI: https://doi.org/10.1016/S0001-8686(98)00035-9

Tu, F., Park, B.J., Lee, D. (2013). Thermodynamically stable emulsions using Janus dumbbells as colloid surfactants. *Langmuir 15*, 12679-12687. DOI: 10.1021/la402897d

Villalobos-Castillejos F., Granillo-Guerrero, V.G., Leyva-Daniel, D.E., Alamilla-Beltrán, L., Gutiérrez-López, G.F., Monroy-Villagrana, A., Mahdi Jafari, S. (2018). Fabrication of nanoemulsions by microfluidization. In: *Nanoemulsions Formulation, Applications, and Characterization*, (McClements, D.J. and Jafari eds.), Pp 207-231. U.S.A. DOI: https://doi.org/10.1016/B978-0-12-811838-2.00008-4

Villalobos-Castillejos, F., Alamilla-Beltrán, L., Monroy-Villagrana, A., Jiménez-Guzmán, J., Dorantes-Álvarez L., and Gutiérrez-López, G.F. (2017). Long term stability of microfluidized emulsions used in microencapsulation by spray drying. *Revista Mexicana de Ingeniería Química 16*, 221-228.

Wagner, C. (1961). Theorie der Alterung von Niederschlagen drch Umlosen (Oswatd-Reifung). Zeitschrift für Elektrochemie. *Berichte der Bunsengesellschaft für physikalische Chemie 65*, 581-591. DOI: https://doi.org/10.1002/bbpc.19610650704

Wais, U., Jackson, A.W., He, T., Zhang, H. (2016). Nanoformulation and encapsulation approaches for poorly water soluble drug nanoparticles. *Nanoscale 8*, 1746-1769. DOI: 10.1039/C5NR07161E.

Wang, B., Adhikari, B., and Barrow, C.J. (2014). Optimization of the microencapsulation of tuna oil in gelatin-sodium hexametaphosphate using complex coacervation. *Food Chemistry 158*, 358-65. DOI: https://doi.org/10.1016/j.foodchem.2014.02.135.

Wang, B., Wang, L.J., Li, D., Adhikari, B., Shi J. (2011). Effect of gum Arabic on stability oil-in-water emulsion stabilized by flaxseed and soybean protein. *Carbohydrate Polymers*, 343-351. DOI: 10.1016/j.carbpol.2011.04.059.

Weiss, J., McClements. (2001). Color changes in hydrocarbon Oil in-Water emulsions caused by Ostwald Ripening. *Journal of Agricultural and Food Chemistry 49*, 4372-4377. DOI: 10.1021/jf010330i.

Whistler, R.L. (2012) *Industrial Gums: Polysaccharides and Their Derivatives*, (James BeMiller and R. Whistler eds.) Academia Press.

Zhao, Y., Khalid, N., Shu, G., Neves, M.A., Kobayashi, I., Nakajima, M. (2017). Formulation and characterization of oil-in-water emulsions stabilized by gelatinized kudzu starch. *International Journal of Food Properties 20*, S1329-S1341. DOI: https://doi.org/10.1080/10942912.2017.1347675.